

Abnormal grain growth in nonequilibrium systems: Effects of point defect patterning

Vasyl O. Kharchenko* and Dmitrii O. Kharchenko

Institute of Applied Physics, National Academy of Sciences of Ukraine, 58 Petropavlovskaya Street, 40000 Sumy, Ukraine

(Received 8 April 2013; published 17 April 2014)

We present a mean-field model for abnormal grain growth processes described by competition of both deterministic and stochastic mechanisms with the grain mobility depending on the grain size. The derived approach is applied to study delayed dynamics of grain growth in system of point defects subjected to irradiation according to the swelling rate theory for irradiated materials. We have shown that with the irradiation dose increase, the corresponding grain growth dynamics is slowed down and growth processes with power-law time asymptotics are realized. We discuss behavior of grain size distributions with competing regular and fluctuation mechanisms.

DOI: [10.1103/PhysRevE.89.042133](https://doi.org/10.1103/PhysRevE.89.042133)

PACS number(s): 05.40.-a, 81.16.Rf, 45.70.Qj, 89.75.Kd

I. INTRODUCTION

It is well known that grain growth dynamics can be governed by different mechanisms, leading to different mathematical approaches of their study. Normal grain growth when grain size evolves as $\langle R(t) \rangle \propto t^{\alpha/2}$, with $\alpha = 1$ can be studied using the Potts model [1] or mean-field or phase-field theories [2]. From experimental observation under normal conditions one can find $\alpha \in [1, \dots, \frac{1}{2}]$ [3,4]. In the mean-field approximation following the Hillert-Mullins (HM) theory it was shown that grain growth can be described by the surface tension of the curved grain boundaries, eliminating stored grain boundary energy [5,6]. This treatment follows the Lifshitz-Slyozov-Wagner (LSW) theory of phase coarsening in dilute systems [7,8]. The corresponding models, known as drift models, take into account deterministic mechanisms only. In stochastic (diffusion) models based on Louat's approach one assumes that the grain boundaries randomly fluctuate [9–14]. From the physical viewpoint it means that atoms located adjacent to grain boundaries can jump from one grain to another in a stochastic manner. Moreover, during grain growth, an individual grain does not grow in an effective average environment because adjacent grains share common boundaries. Generally, in these models the time evolution is considered in the grain size space where the grain size distribution obeys a continuity equation. In the stochastic Mulheran-Harding (MH) theory combining drift and diffusion mechanisms the corresponding evolution is given by the Fokker-Planck equation. From the criticism in Refs. [15–17] it follows that the grain size distributions derived from different theories are controversial even under normal grain size growth. As was shown previously (see Ref. [4] and citations therein) the growth exponent α varies from 1/2 to 2 depending on mechanisms for the grain growth. Moreover, this exponent depends on type of studying materials and can vary with test temperature range.

One should note that abnormal grain growth was studied numerically under normal conditions. In Ref. [18] a problem of abnormal grain growth was considered, studying competing dynamics of small and large grains treated in a sense of multimodal grain size distribution. Here authors used the Hillert radii distribution as initial conditions for the studied system and investigated grain distribution dynamics. It was

shown that abnormal grain growth is associated with rapid growth of a small number of grains whereas the majority of grains do not change their sizes essentially. According to the obtained results it follows that this abnormal grain growth stage stops when small grains are consumed.

The physical picture becomes more complicated when one considers grain growth processes in systems under nonequilibrium conditions, for example, in systems subjected to laser or particle irradiation. From a naive consideration it follows that in irradiated materials, due to defects production in cascades and arrangement of defects with their motion to sinks and diffusion, a deviation from the normal growth with different grain size distributions is possible. For example, in Ref. [19] it was shown that in metallic systems under irradiation one gets the delayed dynamics characterized by $t^{1/5}$. It is principally important that irradiation can enhance mobility of defects and induce stochastic motion of structural elements, leading to realization of all above mechanisms of grain growth. Due to formation of nano-size vacancy and interstitial clusters, vacancies can migrate in the bulk not only toward grain boundaries but also toward clusters of defects emerging inside grains. In such a case the grain growth dynamics can be delayed essentially. Here fluctuation mechanisms of grain growth are able to play a major role in a microstructure evolution. Physically a ballistic mechanism of the diffusion caused by particle irradiation results in a stochastic behavior of diffusivity [20–23]. In such a case with defect production rate increase, macroscopic fluctuations of grain sizes can emerge, resulting in modification of grain morphology. It leads to formation of defect clusters or small grains inside large ones. Therefore, in the problem of grain growth in irradiated systems one should take into account all the above mechanisms incorporated in dynamics of point defect arrangement. In such a case one can expect a competition between diffusion-like mechanism and the mechanism eliminating stored grain boundary energy. Moreover, in such description one should take into account mobility change of the grain boundary caused by motion of defects segregating on these boundaries due to irradiation influence.

In this paper we propose a model for grain growth in nonequilibrium systems, taking into account two above competing mechanisms. In our study the corresponding nonequilibrium conditions are related to irradiation influence, leading to production of defects in solids. In contrast to Ref. [18] we do not use initial grain size distribution; we consider rearrangement of point defects only and relate

*vasiliy@ipfcentr.sumy.ua

the abnormal grain growth to a power-law dependence of the grain radius $\langle R(t) \rangle \propto t^{\alpha/2}$ with $\alpha < 1$. Using the rate theory of defects population evolution, we apply the derived formalism to study numerically dynamics of grains formed by agglomeration of vacancies when they arrange in spatial structure type of grain boundaries and/or individual clusters (see Refs. [24–26]). The time scale for vacancy ensemble evolution is smaller compared to a grain growth time scale, so the vacancy concentration is considered as a fast variable depending on irradiation conditions only. In such a case macroscopic processes of grain growth are studied by means of characteristic size of grains evolving at large time scale. By studying dynamics of the averaged grain area and the corresponding size distribution functions we show that deterministic mechanism of grain growth dynamics is changed by stochastic ones with defect damage rate increases. At small production of defects, a delaying dynamics of grain growth is observed due to the mobility of grain boundaries change, promoting formation of microstructure with grains having small dispersion in sizes. At large defect production rate, when clusters of defects emerge inside grains, stochastic effects start to play an essential role. We propose a model that fits the numerical data well, illustrating different mechanisms of delayed grain growth and the corresponding quasistationary distributions of the grain sizes.

The work is organized as follows. In Sec. II we propose the generalized model for grain growth incorporating deterministic and stochastic dynamics. Here we generalize the well-known MH, LSW, and HM approaches taking into account internal fluctuations satisfying the fluctuation dissipation relation (FDR). Our approach introduces the grain-size-dependent mobility of grain boundary, incorporating well-known mechanism for grain growth and irradiation influence. We show that a self-similar regime of abnormal grain growth is caused by an irradiation effect in a stochastic model with the corresponding multiplicative noise. Section III is devoted to analytical and numerical analysis of the proposed generalized approach. Here we compare analytical results with numerical simulations. In Sec. IV we apply our formalism to study abnormal grain growth and the corresponding grain size distributions, considering a system of point defects according to the swelling rate theory. We conclude in Sec. V.

II. GENERALIZED MODEL FOR THE GRAIN GROWTH

Let us consider the classical model for the grain growth described by the radius of the grain $R \in (0, \infty)$ [27–30]:

$$\begin{aligned} \frac{dR}{dt} &= \mathcal{J}, \\ \mathcal{J} &= \int_0^t \mathcal{D}(R, t, t'; \tau_J) \nabla c(r, t') dt' |_{r=R}, \\ \tau_c \partial_t c &= c_0 - c + \ell^2 \Delta c + K \tau_c, \quad \ell^2 = D_v \tau_c, \end{aligned} \quad (1)$$

where c is the concentration of defects (let us say vacancies) segregating on grain boundaries. Here c_0 is the equilibrium concentration, K is the defect production rate caused by an irradiation influence, ℓ is the diffusion length, τ_c is the time scale for vacancy ensemble evolution, and D_v is the vacancy diffusivity. The diffusion flux \mathcal{J} near the grain

surface corresponds to the velocity of the radius change, where $\mathcal{D}(R, t, t'; \tau_J)$ is the memory kernel (effective diffusivity depending on the grain radius) and τ_J is the relaxation time for the diffusion flux. Time scales τ_c and τ_J are small compared to the corresponding time scale for the grain size evolution. It allows us to consider both defect concentration and diffusion flux as fast variables, taking $\tau_c \partial_t c \simeq 0$ and $\mathcal{J} \rightarrow J(R) \simeq D(R) \nabla c(r) |_{r=R}$. From the first equation in the unscreened domain $r < \ell$ one gets $c(r < \ell) \approx \langle c \rangle - [\langle c \rangle - c_R] \frac{r}{R}$, where $\langle c \rangle = c_0 + K \tau_c$, $c_R = c_\infty (1 + R_s/R)$, $R_s \equiv 2\sigma_0 \Omega / T$; c_∞ , σ_0 , Ω , and T are thermodynamic concentration value near flat surface, surface tension, atomic volume, and temperature, respectively. From this it follows that for the diffusion flux we get $J(R) = \frac{D(R)}{R} (\langle c \rangle - c_R)$. By introducing an effective supersaturation $\Delta = (\langle c \rangle - c_\infty) / c_\infty$ and a critical radius $R_c = R_s / \Delta$ (equivalent to the averaged, i.e., $R_c = \langle R \rangle$) we finally get

$$J(R) = \mu(R) \left(\frac{1}{R_c} - \frac{1}{R} \right); \quad \mu(R) = \frac{c_\infty R_s D(R)}{R}. \quad (2)$$

From classical definitions for both critical radius $R_c^0 = R_s / \Delta_0$ and supersaturation $\Delta_0 = (c_0 - c_\infty) / c_\infty$ we get the relation $R_c = \frac{c_\infty R_s^0 R_c^0}{c_\infty R_s + K \tau_c R_c^0}$, resulting in a decrease of the averaged grain size with the defect generation growth.

Using the obtained formula for the flux, the deterministic dynamics of the grain size is governed by the equation

$$\frac{dR}{dt} = \mu(R) \left(\frac{1}{\langle R \rangle} - \frac{1}{R} \right) \equiv v(R). \quad (3)$$

Let us define a form for the mobility $\mu(R)$. It is well known that dynamics of the system can be slowed down due to the R dependence of the mobility (see Refs. [31–33]). In our case this scenario can be applied directly. Indeed, assuming $\mu(R) = DR^{1+\kappa}$ where $D = \text{const.}$, κ is the scaling exponent, we arrive at the LSW approach with $\kappa = -2$; and with $\kappa = -1$ the HM mechanism is realized.

Considering stochastic dynamics of the grain growth we need to introduce a fluctuation source satisfying FDR. To this end we rewrite Eq. (6) in the form $\dot{R} = -\mu(R) dU/dR$, where the potential is $U(R) = -R/\langle R \rangle + \ln R$. The corresponding fluctuations satisfying FDR are taken in an *ad hoc* form. It results to stochastic dynamics governed by the Langevin equation

$$\dot{R} = -\mu(R) \frac{dU}{dR} + \sqrt{\mu(R)} \xi(t). \quad (4)$$

Here $\xi(t)$ is the Gaussian white noise with an intensity σ^2 proportional to D . The Fokker-Planck equation for the probability density function $\rho(R, t)$ corresponding to the Langevin equation (4) takes the form

$$\frac{\partial \rho}{\partial t} = \frac{\partial}{\partial R} \left[\mu(R) \frac{dU}{dR} + \sigma^2 \frac{\partial}{\partial R} \mu(R) \right] \rho. \quad (5)$$

The system defined by Eqs. (4) and (5) describes evolution of the physical system subjected to the multiplicative noise in the bare potential $U(R)$. In course of time the system attains some equilibrium configuration with $\rho_{\text{eq}}(R) \propto e^{-\Delta G(R)/\sigma^2}$, where ΔG is the potential type of the Gibbs free energy. It means that one can describe the random

motion in the potential ΔG using a thermodynamical approach (see Refs. [34–36]). Indeed, from the entropy variation $\delta S = -\int \delta \rho(R,t) \ln[\rho(R,t)/\rho_{\text{eq}}(R)] dR$ one finds the entropy production $\Sigma = -\int J(R,t) \partial_R \ln[\rho(R,t)/\rho_{\text{eq}}(R)] dR$. This quantity is expressed through the current-force pair. A relation between current and force is given through the Onsager relation: $J(R,t) = -L[R, \rho(R)] \partial_R \ln[\rho(R,t)/\rho_{\text{eq}}(R)]$, where L is the Onsager coefficient. Using a definition $\mu = L/\rho$ from the continuity equation $\partial_t \rho = -\partial_R J$ we get the Fokker-Planck equation describing evolution of ρ in system manifesting a random motion in the potential ΔG as follows: $\partial_t \rho = \partial_R [\mu(\partial_R \Delta G) + \sigma^2 \mu \partial_R] \rho$. As far as the quantity ΔG is initially unknown, next we consider dynamics of the system in the bare potential $U(R)$ studying processes related to Eq. (5).

To describe grain growth processes we have to restrict ourselves with two additional criteria: (i) normalization condition giving the number of grains, i.e., $N(t) \equiv \int \rho(R,t) dR$; and (ii) a conservation of the total area of the system, i.e., $\int dR R^2 \rho(R,t) = S_0$.

A study of time dependencies of the averaged grain size, their numbers, and the corresponding distribution function $\rho(R,t)$ for the system with multiplicative noise is a complicated problem. Therefore, instead of finding the solution of the corresponding Fokker-Planck equation directly next we exploit the standard approach proposed in Ref. [28].

III. SELF-SIMILARITY OF THE SYSTEM

In a self-similar regime considered below for time dependencies one assumes $R(t) \simeq \langle R(t) \rangle = ya(t)$, $\rho(R,t) = a(t)^\gamma \phi(y)$, where the scaling function $a(t) \propto t^H$ is defined through the Hurst exponent $H \in [0, 1]$. From the normalization condition one gets $N(t) \propto [a(t)]^{1+\gamma}$, whereas the conservation law gives $\gamma = -3$. The averaged area of a grain is $\langle s(t) \rangle \simeq \langle R^2(t) \rangle = S_0/N(t)$. Therefore, the time dependence of the averaged grain area $\langle s(t) \rangle$ is quite opposite to the number of grains $N(t)$.

In a quantitative study of the self-similar behavior of the system, let us start from the deterministic model

$$\frac{dR}{dt} = DR^{1+\kappa} \left(\frac{1}{\langle R \rangle} - \frac{1}{R} \right). \quad (6)$$

In further consideration we move to a relative dimensionless radius $u \equiv R/\langle R \rangle$ and introduce an effective time τ defined as

$$\frac{d\tau}{dt} = (1 - \kappa) \langle R \rangle^{\kappa-1}. \quad (7)$$

In such a case instead of Eq. (6) we get an equation for the quantity $u^{1-\kappa}$ as follows:

$$\frac{du^{1-\kappa}}{d\tau} = D(u - 1) - \chi u^{1-\kappa}, \quad (8)$$

where the coefficient χ is

$$\chi \equiv \frac{1 - \kappa}{\langle R \rangle} \frac{d\langle R \rangle}{d\tau}. \quad (9)$$

Following Ref. [28] one should stress that at $\tau \rightarrow \infty$ the quantity χ attains fixed constant value. The right-hand side of Eq. (8) has maximum at $u_m = [\chi(1 - \kappa)/D]^{1/\kappa}$ and takes the corresponding value $-D\{[D/\chi(1 - \kappa)]^{-1/\kappa}(\kappa + 1)\}$. This

function attains zero value at

$$\chi_0/D = (-\kappa)^{-\kappa} (1 - \kappa)^{-(1-\kappa)}. \quad (10)$$

At $\kappa = -2$ one gets the classical result from the Lifshitz-Slyozov theory with $\chi_0/D = 4/27$.

From Eq. (9) one finds a time dependence of the averaged radius in the form

$$\langle R(\tau) \rangle = \exp\left(\frac{\chi\tau}{1 - \kappa}\right). \quad (11)$$

By inserting this result into Eq. (7) we get a relation between physical and effective times:

$$\tau = \frac{1}{\chi} \ln\left(\frac{1 - \kappa}{\chi} t\right). \quad (12)$$

From this one gets an algebraic dependence

$$\langle R(t) \rangle \propto t^H, \quad H = \frac{1}{1 - \kappa}. \quad (13)$$

Obviously, the deterministic equation for the dimensionless radius with the renormalized time $\tau' = \tau/(1 - \kappa)$ takes the form

$$\frac{du}{d\tau'} = Du^\kappa(u - 1) - \chi u, \quad (14)$$

where next we drop the prime for τ' . Stochastic dynamics of u can be obtained from Eq. (14) rewritten in the form $du/d\tau \equiv v(u)$, where the growth velocity $v(u) = Du^\kappa(u - 1) - \chi u$. By introducing notations for mobility $v(u)$ and potential $V(u)$ as

$$v(u) = Du^\kappa, \quad V(u) = u - \frac{u^2}{2} + \frac{\chi}{D} \frac{u^{2-\kappa}}{2 - \kappa} \quad (15)$$

the stochastic dynamics for u is described by the Langevin equation

$$\frac{du}{d\tau} = v(u) + \sqrt{v(u)} \zeta(\tau), \quad v(u) = -v(u) \frac{dV}{du}. \quad (16)$$

Here $\zeta(\tau)$ is the Gaussian white noise with the intensity σ^2 proportional to D .

The Fokker-Planck equation for the corresponding probability density function $P(\tau, u)$ is

$$\partial_\tau P(\tau, u) = -\partial_u [v(u) - \sigma^2 \partial_u v(u)] P(\tau, u). \quad (17)$$

The corresponding solution can be found in the form $P(\tau, u) = \psi(\tau) \phi(u)$. Following the standard approach from LSW theory and taking $\psi(\tau) = \psi(0) e^{-\lambda\tau}$ we obtain two equations: one for time dependence $d\psi(\tau)/d\tau = -\lambda\psi(\tau)$ and another one for $\phi(u)$ in the form

$$\lambda \phi(u) = \{v(u) \phi(u) - \sigma^2 [v(u) \phi(u)]'\}, \quad (18)$$

where a prime denotes a derivative with respect to u . The corresponding solution should be normalized ($\int \phi(u) du = 1$) and two following criteria must be satisfied:

$$\phi(u = 0) = 0, \quad \phi(u \rightarrow \infty) = 0. \quad (19)$$

In the deterministic case ($\sigma^2 = 0$) we arrive at the generalized result with $P(u, \tau) = e^{-\lambda\tau} \phi_0(u)$, where [28]

$$\phi_0(u) = -\frac{N_0 e^{\lambda \tilde{\tau}(u)}}{v(u)}, \quad \tilde{\tau}(u) = \int_0^u \frac{du}{v(u)}.$$

Here N_0 is the normalization constant. Time asymptotics for $\langle R(t) \rangle$ remains the same as shown in Eq. (13), whereas for the number of grains one gets $N(t) \propto t^{-2H}$.

Considering the stochastic case we use a large-noise approximation where $1/\sigma^2$ is a small parameter. Next, the corresponding distribution function we assume in a quasi-Gibbs form $\phi(u) \propto e^{-W(u)/\sigma^2}$. Inserting the proposed solution into Eq. (18) we obtain

$$\lambda = [v - \sigma^2 v' + v W']' - \frac{W'}{\sigma^2} (v - \sigma^2 v' + v W'). \quad (20)$$

In the large noise limit one can neglect the last term in the right-hand side and therefore the approximate solution satisfying conditions (19) takes the form

$$\phi(u) \approx N_0 u^{-\kappa} \exp\left(-\frac{1}{\sigma^2} \left[\frac{\lambda + \chi}{D} \frac{u^{2-\kappa}}{2-\kappa} + u - \frac{u^2}{2} \right]\right). \quad (21)$$

Hence, for the probability density one has $P(u, \tau) = e^{-\lambda\tau} \phi(u)$. Moving back to the distribution $\rho(R, t)$ we get automatically $\gamma = -3$ and $R(t) \propto t^H$ with $s(t) \propto [N(t)]^{-1}$.

In the following study we use the relation $P(u, \tau) du = \rho(R, t) dR$. From the definition $u = R/\langle R \rangle$ the condition of the total area conservation

$$S_0 = e^{-\lambda\tau} \int u^2 \phi(u) du \quad (22)$$

gives the relation

$$\lambda = \frac{2\chi}{1-\kappa}. \quad (23)$$

From the normalization condition for $P(u, \tau)$ and Eq. (23) we get the number of grains

$$N(t) \equiv \int P(u, \tau) du = e^{-\frac{2\chi}{1-\kappa}\tau} \int \phi(u) du. \quad (24)$$

Using the relation between t and τ given by Eq. (12) we obtain

$$N(t) \propto t^{-2H}, \quad (25)$$

where the relation $N(t) = S_0/\langle R(t) \rangle^2$ is satisfied; the Hurst exponent H is defined in Eq. (13). The result given by Eq. (13) can be obtained directly from the definition of the average $\langle u(\tau) \rangle \equiv \int u P(u, \tau) du$.

To make a transition to the grains area distribution we use the relation $\Phi(s, \tau) ds = P(u, \tau) du$ with $s = u^2$. In such a case for the desired quantity we have the quasi-Gibbs distribution

$$\Phi(s, \tau) = N_0 e^{-\lambda\tau} \exp\left(-\frac{U_{ef}(s)}{\sigma^2}\right), \quad (26)$$

where N_0 is the normalization factor and the effective potential is of the form

$$U_{ef}(s) = \frac{\lambda + \chi}{D(2-\kappa)} s^{1-\kappa/2} + s^{1/2} - \frac{s}{2} + \frac{\sigma^2(\kappa + 1)}{2} \ln s. \quad (27)$$

It is interesting to note that in the problem under consideration multiplicative noise is able to induce nonequilibrium transitions with modality change of the distribution function [37], where macroscopic phases relate to positions of corresponding

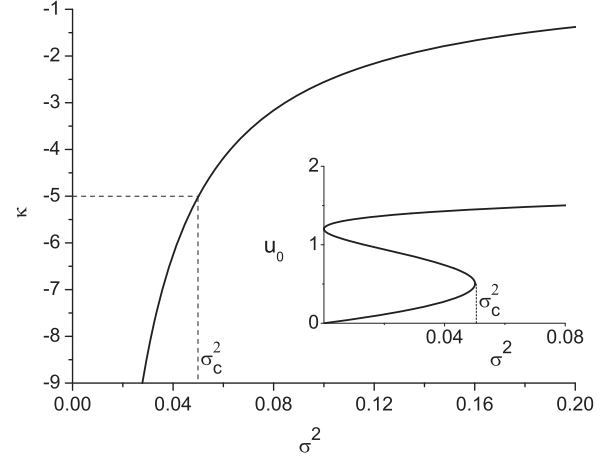


FIG. 1. Phase diagram for noise-induced transitions.

maxima. The role of multiplicative noise in noise-induced nonequilibrium phase transitions in spatially extended systems was considered previously (see, for example, Refs. [38–41] and citations therein) where it was shown that the multiplicative noise is able to induce formation of phases treated in the thermodynamical sense in spatially extended systems. Usually, noise-induced nonequilibrium transitions are studied in the stationary limit, i.e., at $t \rightarrow \infty$. In such a case the stationary distribution $P_s(u) = P(\tau \rightarrow \infty, u)$ coincides with $\phi(u)$ from Eq. (21) where one should put $\lambda = 0$. It should be noted that $P_s(u)$ obtained at conditions of zero fluxes on boundaries of stochastic process $u(\tau)$ reduced to an equilibrium distribution $P_{eq}(u) \propto e^{-\Delta G(u)/\sigma^2}$ with $\Delta G(u) = V(u) - \sigma^2 \ln v(u)$ and $P_{eq}(u=0) = P_{eq}(u=\infty) = 0$. In such a case we have a generalization of the models with logarithmic and power-law forms for the thermodynamic potential $\Delta G(u)$ proposed in Ref. [35]. The corresponding diagram illustrating modality change of the distribution $P_{eq}(u)$ at noise-induced transitions is shown in Fig. 1. Here at $\sigma^2 < \sigma_c^2$ one has bimodal distribution over grain sizes (see insertion for the most probable value u_0 vs σ^2). Above the critical value σ_c^2 one has unimodal distribution.

To verify the approximation for the grain size distribution (21) we perform simulations of the Langevin equation (16) on the graphical processor units (GPUs) with double precision. This technique provided an effective acceleration of numerics by a factor of about 300 over the standard CPUs computing for this problem. Time step was $\Delta\tau = 10^{-3}$. The corresponding probability density functions (PDF) $\phi(u)$ at different κ and elevated noise intensities σ^2 are shown in Fig. 2. Here solid, dashed, and dotted curves correspond to analytical approximation (21) with χ and λ taken from Eqs. (10) and (23) at $(\sigma^2 = 10, \kappa = -4)$, $(\sigma^2 = 5, \kappa = -2)$, $(\sigma^2 = 10, \kappa = -2)$, respectively. The insertion indicates temporal behavior of the averaged quantity $\langle u \rangle$ at the same system parameters. It is seen that at large $|\kappa|$ both the most probable value u_0 and $\langle u \rangle$ take lower values (cf. triangles and circles with corresponding curves). From the obtained data one finds that internal fluctuations lead to the same effect. Comparing numerics with analytical approximation we arrive at the conclusion that the good correspondence between these two

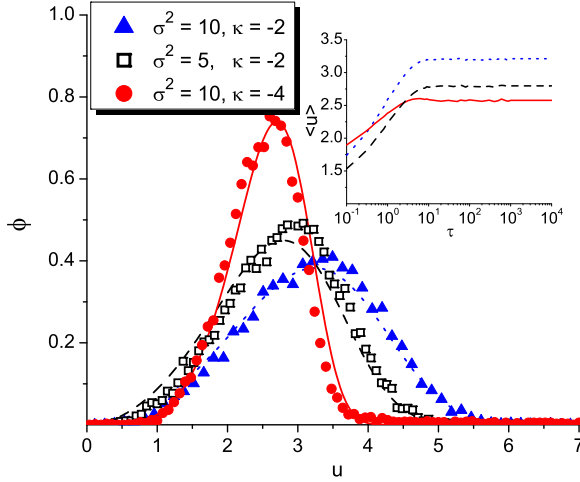


FIG. 2. (Color online) Probability density functions $\phi(u)$ at the large noise limit at different κ . Symbols correspond to numerical results; lines relate to the analytical approximation given in Eq. (21).

approaches is observable at large noise limit (cf. triangles and circles with squares and the corresponding curves).

In the next section we apply the derived formalism to study anomalous grain growth with the corresponding universality and scaling in irradiated systems using an independent model for the point defects evolution.

IV. APPLICATION: UNIVERSALITY OF GRAIN GROWTH IN IRRADIATED SYSTEMS

A. Model of point defects evolution

Using the standard approach of the rate theory [42] the dynamics of point defects in irradiated systems is described by a two-component model:

$$\partial_t c_{v,i} = K - D_{v,i} S_{v,i} c_{v,i} - \alpha c_v c_i. \quad (28)$$

Here $c_{v,i}$ correspond to population of vacancies (v) and interstitials (i), respectively. The first term in Eq. (28) relates to the displacement damage rate and takes into account a production of defects due to irradiation influence. The second term describes the effect of sinks (S_i and S_v) related to bias factors $Z_{i,v}$, network dislocation density ρ_N , vacancy ρ_v , and interstitial ρ_i loop densities as follows: $S_{\{v,i\}} = Z_{\{v,i\}N} \rho_N + Z_{\{v,i\}V} \rho_v + Z_{\{v,i\}I} \rho_i$, where $Z_{vN,vI,vV} = 1$, $Z_{iN} = 1 + B$, $Z_{iI} \simeq Z_{iV} \simeq 1 + B'$, $B' \geq B$, $B \simeq 0.1$; $D_{v,i}$ represent the corresponding diffusivities. The last term governs nonlinear contribution caused by point defect annihilation with the recombination coefficient $\alpha = 4\pi r_0 (D_i + D_v) / \Omega$ given in terms of recombination radius r_0 and atomic volume Ω .

In metallic systems due to large difference between migration energies of point defects one can introduce small parameter $\nu \equiv D_v/D_i \ll 1$ and eliminate adiabatically fast variable c_i . Using renormalized quantities $S_{v,i} = Z_{\{v,i\}N} \rho_N (1 + \rho_v^* + \rho_i^*)$, $\rho_{v,i}^* \equiv \rho_{v,i} / \rho_N$, $t' \equiv t \lambda_v$, $\lambda_v \equiv D_v Z_{vN} \rho_N$, $x_{\{i,v\}} = \gamma C_{\{i,v\}}$, $\gamma \equiv \alpha / \lambda_v$, $\eta \equiv (1 + \rho_v^* + \rho_i^*)$, $Z_{iN}/Z_{vN} = 1 + B$ with $K' \equiv \gamma K / \lambda_v$ measured in units of displacement per atom, the system (28) is reduced to $\partial_t x = K - \eta x - K \nu x / [\eta(1 + B) + \nu x]$, where x relates to the vacancy concentration (we drop all

primes). Here the last term is related to the nonlinearity caused by influence of interstitials. Following previous studies (see Refs. [24–26,43]) we incorporate a production of defects by elastic field caused by defect presence. This effect is described by introduction the term $G \exp[\varepsilon x / (1 + x^2)]$ into dynamical equation for x , where $\varepsilon \equiv 2Z E_0^e / T$ is defined through the defect formation energy E_0^e , temperature T , and coordination number Z ; the renormalized constant G is proportional to probability of defects generation by the elastic field.

As far as vacancies are mobile species next we have to introduce their flux. It contains pure diffusion part $-L_d^2 \nabla x$ with diffusion length $L_d^2 \equiv D_v / \lambda_v$ and the component describing defects interaction $\mathbf{v}x = -(L_d^2 / T) x \nabla U$. For the interaction potential we assume self-consistency relation [24,44–46] $U = -\int \tilde{u}(r, r') x(r') dr'$, where $-\tilde{u}(r)$ is the attraction potential with properties $\int \tilde{u}(r) r^{2n+1} dr = 0$. Assuming that $x(r)$ does not change essentially on the distance $r_0 \simeq \Omega^{1/3}$, one can use an expansion

$$\frac{1}{T} \int d\mathbf{r}' \tilde{u}(\mathbf{r} - \mathbf{r}') x(\mathbf{r}') \simeq \varepsilon (x + r_0^2 \nabla^2 x), \quad (29)$$

where the first term leads to the well-known relation between the elastic field potential and the concentration of defects $U = -\kappa \varpi \nabla \cdot \mathbf{u}$; for the displacement vector \mathbf{u} one has $\nabla \cdot \mathbf{u} \propto \varpi x$, κ is the elastic constant, and ϖ is the dilatation parameter [47]. The second part in Eq. (29) is responsible for microscopic processes of defect interactions in the vicinity of the interaction radius r_0 . Under normal conditions this term is negligibly small compared to the ordinary diffusion one. In the absence of the second term in Eq. (29) for the flux one gets $\mathbf{J} \propto -(1 - \varpi \kappa x / T) \nabla x$, where the concentration depending diffusion coefficient $(1 - \varpi \kappa x / T)$ can be negative at some interval for x . It means that a homogeneous distribution of defects starting from some critical speed of its formation related to the temperature, sinks density, and dilatation volume becomes unstable. The emergence of the directional flux of defects results in supersaturation of vacancies and formation of clusters or voids. From a mathematical viewpoint such divergence appearing at short time scales cannot be compensated by nonlinear part of the reaction terms. The second term in expansion (29) can prevent such divergence and, therefore, it must be retained. In such a case dynamics of vacancies is governed by the equation

$$\partial_t x = f(x) - \nabla \cdot \mathbf{J} \quad (30)$$

with the reaction term

$$f(x) \equiv K - \eta x - \frac{K \nu x}{\eta(1 + B) + \nu x} + G \exp\left(\frac{\varepsilon x}{1 + x^2}\right) \quad (31)$$

and the diffusion flux

$$\mathbf{J} \equiv -[\nabla x - \varepsilon x \nabla(x + \ell^2 \nabla^2 x)]. \quad (32)$$

Here we have used renormalized quantities: $\mathbf{r}' = \mathbf{r} / L_d$, $\ell = r_0 / L_d$, $r_0 \ll L_d$. As was shown in Refs. [24–26,43] an introduction of the last term in $f(x)$ results in a bimodal behavior of the homogeneous stationary state x_s at elevated ε and small K . The corresponding phase diagram and the related dependence $x_s(K)$ are shown in Fig. 3 where K_{b1} and

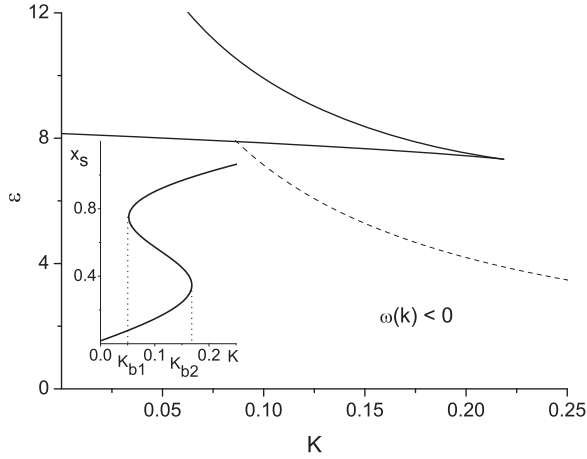


FIG. 3. Phase diagram for the homogeneous system at $\varepsilon = 10.5$, $\eta = 1$, $\nu = 10^{-2}$, $G = 0.015$. Insertion is given at $\varepsilon = 8$.

k_{b2} correspond to binodals (see insertion in Fig. 3). At large K there is a unique state with high vacancy concentration.

From the stability analysis of the homogeneous states it follows that a behavior of inhomogeneous perturbations is described by the dispersion relation

$$\omega(k; x_s) = -k^2[1 - \varepsilon x_s(1 - \ell^2 k^2)]. \quad (33)$$

It follows that unstable modes (with $\omega(k) > 0$) are characterized by wave numbers $0 < k < k_c$, where $k_c = \sqrt{\frac{\varepsilon x_s - 1}{\varepsilon x_s \ell^2}}$ is defined through the condition $\omega(k) = 0$. The dashed line in Fig. 3 corresponds to the condition $\omega(k) = 0$. It is seen that in the simplest case of $\ell \rightarrow 0$ in monostable domain (below the cusp) all states with $x_s > 1/\varepsilon$ are unstable with respect to inhomogeneous perturbations with $k_c \rightarrow \infty$, whereas states with $x_s < 1/\varepsilon$ are stable. In the actual case $\ell \neq 0$ the system states characterized by $x_s > 1/\varepsilon$ are unstable with wave numbers lying in the interval $0 < k < k_c$. In the bimodal domain the system is always unstable with respect to inhomogeneous perturbations. The wave number for the most unstable mode k_0 can be found from the solution of the equation $d\omega(k)/dk = 0$. It follows that $k_0 = k_c/\sqrt{2}$.

A corresponding Langevin dynamics can be considered introducing a random source satisfying the fluctuation dissipation relation. Acting in the standard manner we rewrite original deterministic model in the form

$$\partial_t x = f(x) + \nabla \cdot M(x) \nabla \mu, \quad \mu \equiv \frac{\delta \mathcal{F}}{\delta x}, \quad (34)$$

where $M(x) = x$, and for the free energy functional $\mathcal{F}[x]$ we have

$$\mathcal{F}[x] = \int d\mathbf{r} \left[x \ln x - x - \frac{\varepsilon}{2} x^2 + \frac{\varepsilon \ell^2}{2} (\nabla x)^2 \right]. \quad (35)$$

Formally, Eq. (34) can be represented in the canonical form

$$\partial_t x = -\frac{1}{M(x)} \frac{\delta \mathcal{U}}{\delta x}, \quad (36)$$

where for the functional $\mathcal{U}[x]$ we know only its first derivative, i.e.,

$$\delta \mathcal{U} = - \int d\mathbf{r} \delta x [M(x)R(x) + M(x)\nabla \cdot (M(x)\nabla \mu)]. \quad (37)$$

Following Refs. [45,48–51] we can introduce a fluctuation source obeying fluctuation-dissipation relation in an *ad hoc* form:

$$\partial_t x = -\frac{1}{M(x)} \frac{\delta \mathcal{U}}{\delta x} + \sqrt{\frac{1}{M(x)}} \xi(\mathbf{r}, t), \quad (38)$$

where ξ is the white noise with

$$\langle \xi(\mathbf{r}, t) \rangle = 0, \quad \langle \xi(\mathbf{r}, t) \xi(\mathbf{r}', t') \rangle = 2\tilde{\sigma}^2 \delta(\mathbf{r} - \mathbf{r}') \delta(t - t'); \quad (39)$$

$\tilde{\sigma}^2$ is the noise intensity, proportional to the bath temperature.

As was shown in our previous studies (see Refs. [24,25]) the internal multiplicative noise leads to instability of the homogeneous states at short time scales, whereas inhomogeneous perturbations is described by dependence shown in Eq. (32).

B. Numerical results and discussion

We study the dynamics of pattern formation numerically on a CPU, on two-dimensional grid with 1024×1024 sites and periodic boundary conditions with phase space $x \in [0, 1]$, in order to suppress amorphization characterized by extremely large amount of defects. In our simulations we take time step $\Delta t = 2.5 \times 10^{-4}$, and the mesh size is $\Delta l = 0.5$; $\ell = 0.5$. For initial conditions we take $\langle (\delta x(\mathbf{r}, 0))^2 \rangle = 0.1$. Using the obtained dynamical phase diagram (see Fig. 3 in Ref. [24]) and fixing $\varepsilon = 10.5$ we consider only regimes when defects segregate on grain boundaries and arrange into clusters inside grains, and we investigate dynamics of grain growth with variation in defect damage rate K . To this end we study temporal behavior of the average grain area $\langle s(t) \rangle$, their population $\langle N(t) \rangle$, and the stationary probability density functions of grain sizes. System parameters used in simulations are: $\varepsilon = 10.5$, $\eta = 1$, $\nu = 10^{-2}$, $G = 0.015$.

Typical snapshots of the system evolution at different values of damage rate K are shown in Fig. 4. It is seen that at small K [see column (a)] starting from a homogeneous distribution of the field x point defects organize in extended structure type of walls of defects forming grain boundaries of different sizes. During the system evolution grains having fewer than six sides disappear, as was predicted by von Neumann [52] and Mullins [6]. Here for the area of the grain s_n with n sides the well-known law $ds_n/dt = M(n - 6)$ is satisfied ($M = \text{const.}$). Following the HM approach one has a relation between n and grain radius as follows: $n \propto R/\langle R \rangle$, where $\langle R \rangle$ is the mean grain size. In such a case the curvature driven mechanism for the grain growth is applicable. At elevated K [see column (b) in Fig. 4] due to large defect production a microstructure is changed. Here clusters of defects emerge inside growing grains. In such a case vacancies produced in cascades are able to migrate to sinks like grain boundaries and to jump to other grains. They can move to other sinks, namely, vacancy clusters inside grains. This leads to a probabilistic migration of defects resulting in Langevin dynamics of the grain growth relevant to Louat's

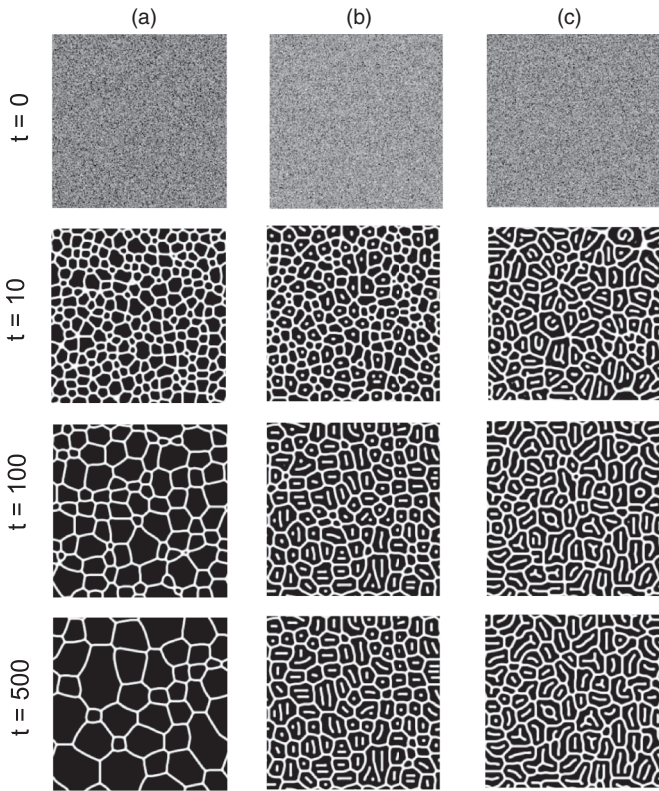


FIG. 4. Snapshots of the deterministic system evolution at $K = 0.05$ (a), $K = 0.15$ (b) and $K = 0.225$ (c). In order to illustrate the microstructure we present the system of 256×256 sites.

approach. With a further increase in the defect damage rate a special type of diffusion having athermal character (ballistic diffusion) is realized due to the large number of cascades in the system. It results in structural disorder with large amount of vacancies. They are attracted by clusters inside grains that lead to formation of extended clusters due to interactions between them. Such evolution scenario results in formation of microstructure when small grains emerge inside large ones [see Figs. 4(c) and 5 as typical crops]. Therefore, here one has macroscopic fluctuations of grain morphology where the derived approach in the previous section cannot be applied directly.

It is interesting to compare a corresponding microstructure change for deterministic and stochastic systems. It is known that the noise can change a scenario of pattern formation comparing with the deterministic case (see, for example, Refs. [38,53–55] and citations therein). In Fig. 6 snapshots of patterns obtained at different defect production rates and noise intensities are shown. It is seen that the noise acts in the



FIG. 5. Typical microstructure of grains shown in Fig. 4(c) as crops from snapshots in system with 1024×1024 sites.

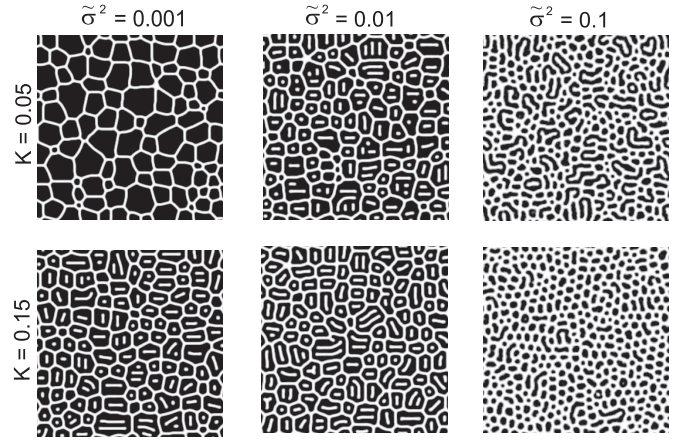


FIG. 6. Typical patterns observed at different defect production rate K and noise intensities $\tilde{\sigma}^2$.

same manner as defect production rate; i.e., with increase in $\tilde{\sigma}^2$ defects inside grains emerge. At elevated noise intensities we get large amount of grains with small sizes. Detailed study of stationary patterns obtained at different noise intensities was reported in Refs. [24,25].

Next, let us study dynamics of the averaged grain area $\langle s \rangle$ and number of grains $\langle N \rangle$ varying the damage rate K , where averages are taken over the system and the number of numerical experiments. In our study we use 15 runs. The corresponding dependencies are shown in Fig. 7 in log-log plot at fixed value of K . It is seen that there are two stages of the system evolution. The first stage relates to the grain growth dynamics. The second one corresponds to stationary case when a microstructure of the system is not changed. It is principally important that the second regime is possible only if $K \neq 0$, which differs from ordinary annealed system where grains grow constantly (normal conditions). Next we study only the regime of the grain growth. From our numerical data it follows that the regime of grain growth is characterized by power-law dependencies: $\langle s(t) \rangle \propto t^\alpha$ and $\langle N(t) \rangle \propto t^{-\tilde{\alpha}}$ with $\alpha/\tilde{\alpha} \simeq 1$ and the estimation error is less than 5%. We have found that the scaling exponent α falls down with an increase in K (see Fig. 8). Formally, in the limit $K \rightarrow 0$ the growth exponent tends to the classical value $\alpha \rightarrow 1$ of the HM scenario for the grain growth. An increase in K leads to delaying the grain

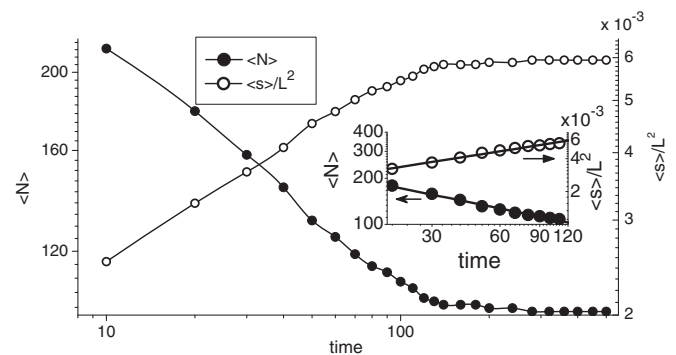
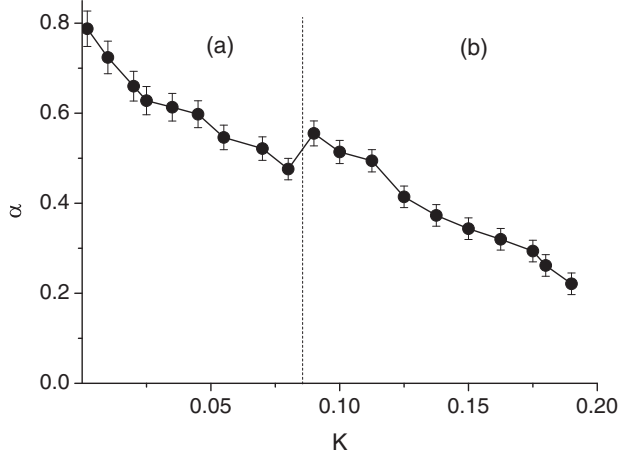
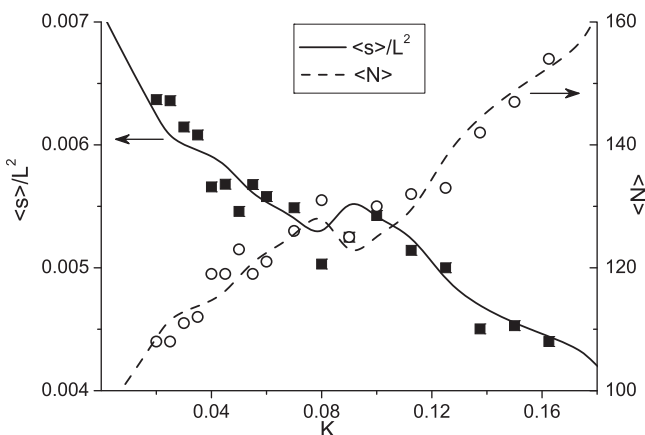
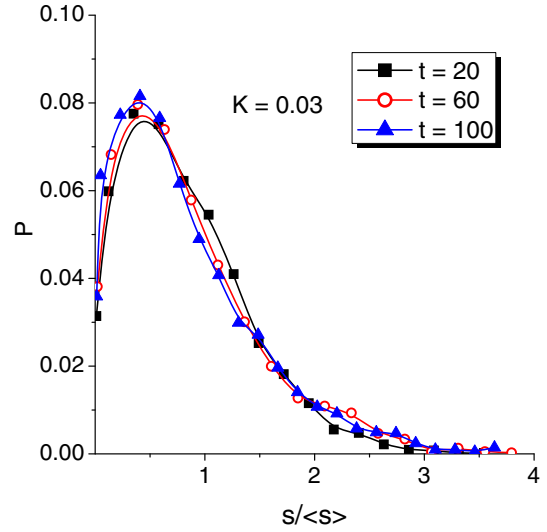


FIG. 7. Dynamics of both number of grains and averaged area of grains at $K = 0.15$.


 FIG. 8. Scaling exponent α vs damage rate K .

growth dynamics caused by formation of defects inside grains violating curvature-driven mechanism. The nonmonotonic decrease of the dependence $\alpha(K)$ allows one to find two domains separated by a kink. In the domain (a) one gets grains free of vacancy clusters. The domain (b) is characterized by microstructure with grains having defect clusters. Moreover, transition from the domain (a) toward domain (b) relates to modality change of the stationary homogeneous state (see phase diagram in Fig. 3). The transition point well corresponds to the point K_{b2} from the second binodal in the space (K, ε) for $\varepsilon = 10.5$.

Considering a behavior of both grain size and number of grains vs defect damage rate K at fixed times, one can find relations $\langle s(K) \rangle \propto e^{\alpha(K)}$, $N(K) \propto e^{-\alpha(K)}$. It means that following the obtained decreasing dependence $\alpha(K)$ the averaged area of grains becomes smaller when K increases, whereas the number of grains grows. The result of the grain size decrease with growth in K was shown analytically in the previous section. The independent calculations of the averaged grain size area and the number of grains at fixed time shown in Fig. 9 well correspond to obtained exponential dependencies vs K . Here symbols correspond to direct calculations of $\langle s(K) \rangle$


 FIG. 9. Averaged grain area and number of grains vs K at time fixed time $t = 50$.

 FIG. 10. (Color online) Universality of the probability density function of the grain size distribution at different times at $K = 0.03$.

and $\langle N(K) \rangle$, whereas lines relate to dependencies $e^{\pm\alpha(K)}$ from the data shown in Fig. 8.

Let us analyze the probability density function (PDF) of the grain sizes at different times. As Fig. 10 shows, one has a universal behavior for $P(s/\langle s \rangle)$. Therefore, the independence of PDF in time and scaling law asymptotics of $\langle s(t) \rangle$ and $\langle N(t) \rangle$ characterize a self-similarity of the system dynamics.

Let us consider probability density over grains area at different rates K . To fit data at fixed K we use the formalism presented in the previous section for the grain area. First, we determine the corresponding value for the exponent α from data shown in Fig. 8. Next, using the relation $\alpha = 2H$ where the Hurst exponent is given by Eq. (13) we can define the exponent κ for the mobility $\mu(u)$. Using value of κ we obtain χ and λ from Eqs. (10) and (23). To fit the obtained data we use the approximation (26) with fitting parameters D , N_0 , and σ^2 . The corresponding results are shown in Fig. 11. It is seen that at small rates K the most probable grain area is less than the averaged area $\langle s \rangle$ (see left panel), whereas at elevated K most of grains are characterized by the mean area (see right panel). Therefore, an increase in K results not only in grain number growth but also in equalizing grain sizes. It should be noted that the derived formalism for the grain size distribution works well in the vicinity of the main peak related to the most probable value of the grain area. However, the correspondence between analytical results and numerical data is better for elevated K related to large noise intensities σ^2 . This statement is expected due to the analytical

 TABLE I. Fitting parameters for PDF's at different K .

K	D	σ^2	$\Sigma \equiv \sigma^2/D$
0.03	0.24 ± 0.01	0.26 ± 0.01	1.08
0.05	0.2 ± 0.01	0.27 ± 0.01	1.35
0.15	0.1 ± 0.01	0.7 ± 0.01	7.03

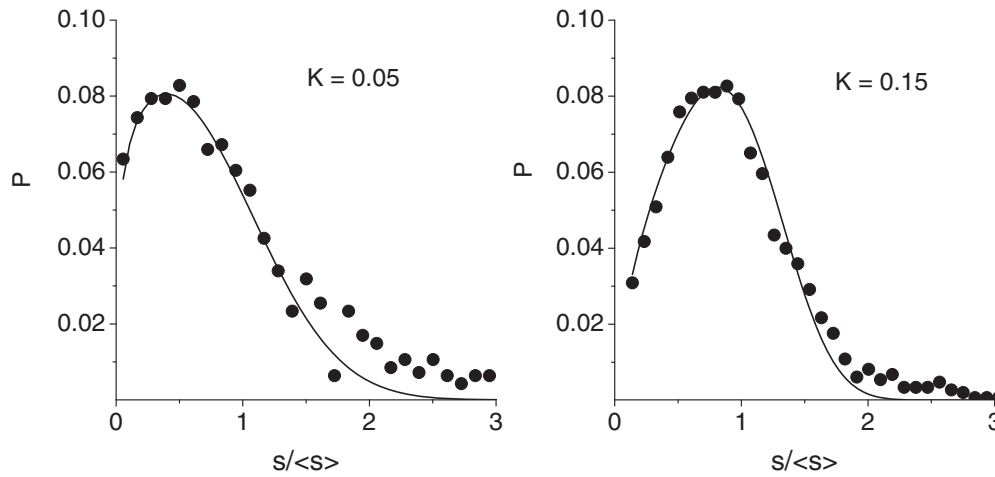


FIG. 11. Probability density functions at different damage rates K .

treatment done for the large noise limit. From the obtained data one gets that at large K the main contribution to the grain size dynamics is governed by the stochastic component with Louat’s grain growth mechanism, whereas at small K the deterministic component relevant to MH approach plays a major role (see system parameters in Table I). Here the value of the diffusion constant D decreases with K growth in the fitting procedure, whereas σ^2 takes elevated values. As far as the noise intensity σ^2 is proportional to D one can estimate the pure stochastic contribution introducing a parameter characterizing fluctuations as $\Sigma \equiv \sigma^2/D$ (see third column in Table I). It increases dramatically at large K corresponding to transition from bimodal toward unimodal system states (see Fig. 3).

One can expect that a further increase in K will lead to better correspondence of the numerical data with analytical predictions. At the same time, as was shown previously, when K takes larger values a picture of point defects self-organization becomes more complicated due to formation of small grains inside large ones [see snapshots in Fig. 4(c) and crops in Fig. 5]. Such rearrangement of defect structure can lead to fragmentation of grains. Unfortunately, the derived formalism for the grain growth is unable to describe these processes and will be considered elsewhere.

V. CONCLUSIONS

We proposed a generalized mathematical model for the grain growth which takes into account main deterministic and stochastic contributions of the system evolution. It is shown that due to grain-size-dependent mobility the dynamics of grain growth can be essentially delayed. We have shown that the system manifests self-similar dynamical regime, where the corresponding growth exponent dependson the model for the mobility. We obtain a general construction for the

grain size distribution in deterministic model. Considering stochastic dynamics we found the grain size distribution in the limit of large fluctuations and we verified it using a simulation procedure that gave good agreement with analytical predictions.

The derived formalism was applied to study grain growth considering spatial arrangement of point defects in an independent model of irradiated system using the swelling rate theory. It was shown that a good agreement between analytical results and numerical simulations in such a system is realized under the assumption of grain-size-dependent mobility. By studying self-organization of vacancies segregating on grain boundaries we have shown that a competition between both deterministic and stochastic mechanisms is realized in irradiated systems. It was found that at small defect damage rate the main role in system dynamics is played by the regular part of the grain growth velocity that corresponds well to Hillert-Mullins or Lifshitz-Slyozov-Wagner theories. At elevated defect production rates the stochastic contribution (Louat’s mechanism) caused by grain-size-dependent mobility starts to play a major role in the system evolution. Analytical predictions related to a decrease of the grain size with an increase in the defect production rate are in agreement with independent simulations of point defects dynamics. It was shown that at elevated damage rate caused by irradiation influence most of grains equalize their sizes with an increased number of grains.

The derived formalism can be exploited to study grain growth, void formation, or formation and dissolution of precipitates in materials under laser or particle irradiation. We expect that nontrivial results obtained in this work will stimulate a further study of grain growth dynamics in condensed matter systems under nonequilibrium conditions, for example, under particle or laser irradiation.

[1] M. P. Anderson, D. J. Srolovitz, G. S. Crest *et al.*, *Acta Metall.* **32**, 783 (1984).
 [2] D. Fan and L. Q. Chen, *Acta Mater.* **45**, 611 (1997).

[3] P. Mulheran and J. H. Harding, *Acta Metallurgica* **39**, 2251 (1991).
 [4] H. V. Atkinson, *Acta Metall.* **36**, 469 (1988).

- [5] M. Hillert, *Acta Metall.* **13**, 227 (1965).
- [6] W. W. Mullins, *Acta Mater.* **46**, 6219 (1998).
- [7] I. M. Lifshitz and V. V. Slyozov, *J. Phys. Chem. Solids* **19**, 35 (1961).
- [8] C. Wagner, *Z. Elektrochem.* **65**, 581 (1961).
- [9] N. P. Louat, *Acta Metall.* **22**, 721 (1974).
- [10] C. S. Pande, *Acta Metall.* **35**, 2671 (1987).
- [11] I. W. Chen, *Acta Metall.* **35**, 1723 (1987).
- [12] C. S. Pande and E. Dantsker, *Acta Metall.* **38**, 945 (1990).
- [13] C. S. Pande and E. Dantsker, *Acta Metall.* **42**, 2899 (1994).
- [14] C. S. Pande, R. A. Masumara, and S. P. Marsh, *Philos. Mag. A* **81**, 1229 (2001).
- [15] N. Ryum and O. Hunderi, *Acta Metall.* **37**, 1375 (1989).
- [16] K. W. Wang, *Z. Phys. B* **99**, 593 (1996).
- [17] I. A. Ovid'ko, *Fiz. Mekh. Mater.* **8**, 174 (2009).
- [18] J. Svoboda and F. D. Fischer, *Modell. Simul. Mater. Sci. Eng.* **22**, 015013 (2014).
- [19] A. V. Barashev and S. I. Golubev, *J. Nucl. Mater.* **389**, 407 (2009).
- [20] V. I. Dubinko, A. V. Tur, A. A. Turkin, and V. V. Yanovsky, *Radiat. Eff.* **112**, 233 (1990).
- [21] D. O. Kharchenko, I. O. Lysenko, and S. V. Kokhan, *Eur. Phys. J. B* **76**, 37 (2010).
- [22] D. Kharchenko, I. Lysenko, and V. Kharchenko, *Phys. A (Amsterdam, Neth.)* **389**, 3356 (2010).
- [23] D. Kharchenko, V. Kharchenko, and I. Lysenko, *Cent. Eur. J. Phys.* **9**, 698 (2011).
- [24] V. O. Kharchenko and D. O. Kharchenko, *Eur. Phys. J. B* **85**, 383 (2012).
- [25] V. O. Kharchenko and D. O. Kharchenko, *Condens. Matter Phys.* **16**, 33001 (2013).
- [26] D. O. Kharchenko, V. O. Kharchenko, A. I. Bashtova, *Ukr. J. Phys.* **58**, 993 (2013).
- [27] L. D. Landau and E. M. Lifshitz, *Statistical Physics, Part 1* (3rd ed.) (Elsevier Butterworth-Heinemann, Oxford, 1980), Vol. 5.
- [28] L. P. Pitaevskii and E. M. Lifshitz, *Physical Kinetics* (Pergamon Press, Oxford, 1981), Vol. 10.
- [29] L. A. Maksimov and A. I. Ryazanov, *Sov. Phys. JETP* **52**, 1170 (1980).
- [30] A. I. Olemskoi and A. Ya. Flat, *Phys. Solid State* **35**, 278 (1993).
- [31] C. L. Emmott and A. J. Bray, *Phys. Rev. E* **59**, 213 (1999).
- [32] D. O. Kharchenko, *Fluct. Noise Lett.* **2**, L273 (2002).
- [33] D. O. Kharchenko and A. V. Dvornichenko, *Phys. A (Amsterdam, Neth.)* **387**, 5342 (2008).
- [34] D. Reguera, J. M. Rubi, and A. Perez-Madrid, *Phys. A (Amsterdam, Neth.)* **259**, 10 (1998).
- [35] J. M. Rubi and A. Gadomski, *Phys. A (Amsterdam, Neth.)* **326**, 333 (2003).
- [36] J. M. Rubi, *Phys. Scr. T* **151**, 014027 (2012).
- [37] W. Horsthemke and R. Lefever, *Noise-Induced Transitions* (Springer-Verlag, New York, 1984).
- [38] J. Garcia-Ojalvo and J. M. Sancho, *Noise in Spatially Extended Systems* (Springer-Verlag, New York, 1999).
- [39] C. Van den Broeck, J. M. R. Parrondo, and R. Toral, *Phys. Rev. Lett.* **73**, 3395 (1994).
- [40] S. Ciuchi, F. de Pasquale, and B. Spagnolo, *Phys. Rev. E* **47**, 3915 (1993).
- [41] A. I. Olemskoi, D. O. Kharchenko, and I. A. Knyaz, *Phys. Rev. E* **71**, 041101 (2005).
- [42] D. Walgraef, *Spatio-temporal Pattern Formation* (Springer-Verlag, New York, 1996).
- [43] F. Kh. Mirzoev, V. Ya. Panchenko, and L. A. Shelepin, *Tech. Phys. Lett.* **22**, 28 (1996).
- [44] D. Batogkh, M. Hildebrant, F. Krischer, and A. Mikhailov, *Phys. Rep.* **288**, 435 (1997).
- [45] D. O. Kharchenko, S. V. Kokhan, and A. V. Dvornichenko, *Phys. D (Amsterdam, Neth.)* **238**, 2251 (2009).
- [46] D. O. Kharchenko, S. V. Kokhan, and A. V. Dvornichenko, *Metallofiz. Noveishie Tekhnol.* **31**, 23 (2009).
- [47] F. Kh. Mirzoev, V. Ya. Panchenko, and L. A. Shelepin, *Phys. Usp.* **39**, 1 (1996).
- [48] S. E. Mangioni, R. R. Deza, and H. S. Wio, *Phys. Rev. E* **63**, 041115 (2001).
- [49] V. O. Kharchenko, *Phys. A (Amsterdam, Neth.)* **388**, 268 (2009).
- [50] B. von Haefthen, G. Izús, S. Mangioni, A. D. Sánchez, and H. S. Wio, *Phys. Rev. E* **69**, 021107 (2004).
- [51] S. E. Mangioni and H. S. Wio, *Phys. Rev. E* **71**, 056203 (2005).
- [52] J. von Neumann, *Metal Interfaces* (American Society for Metals, Cleveland, OH, 1952), p. 108.
- [53] M. Cross and H. Greensidem, *Pattern Formation and Dynamics in Nonequilibrium Systems* (Cambridge University Press, Cambridge, 2009).
- [54] D. Valenti, A. Fiasconaro, and B. Spagnolo, *Acta Phys. Pol. B* **35**, 1481 (2004).
- [55] A. Fiasconaro, D. Valenti, and B. Spagnolo, *Acta Phys. Pol. B* **35**, 1491 (2004).